Croal, Paula L. and Driver, Ian D. and Francis, Susan T. and Gowland, Penny A. (2016) Field strength dependence of grey matter R2* on venous oxygenation. NeuroImage . ISSN 1095-9572

Field strength dependence of grey matter R_2^* on venous oxygenation

Paula L. Croal, Ian D. Driver, Susan T. Francis, Penny A. Gowland

PII: S1053-8119(16)30552-3
DOI: http://dx.doi.org/10.1016/j.neuroimage.2016.10.004
Reference: YNIMG13501

To appear in: *NeuroImage*

Received date: 12 April 2016
Revised date: 19 September 2016
Accepted date: 1 October 2016

Cite this article as: Paula L. Croal, Ian D. Driver, Susan T. Francis and Penny A Gowland, Field strength dependence of grey matter R_2^* on venous oxygenatior *NeuroImage,* http://dx.doi.org/10.1016/j.neuroimage.2016.10.004

Field strength dependence of grey matter R_2^* on venous oxygenation

Paula L. Croal[1], Ian D. Driver[1], Susan T. Francis[1], Penny A. Gowland[1*]

Sir Peter Mansfield Imaging Centre, School of Physics and Astronomy, University of Nottingham, UK.

*Corresponding Author: Sir Peter Mansfield Imaging Centre, School of Physics and Astronomy, University of Nottingham, Nottingham, NG7 2RD, Tel: 0115 9514747. Email: penny.gowland@nottingham.ac.uk

Abstract

The relationship between venous blood oxygenation and change in transverse relaxation rate (ΔR_2^*) plays a key role in calibrated BOLD fMRI. This relationship, defined by the parameter **β,** has previously been determined using theoretical simulations and experimental measures. However, these earlier studies have been confounded by the change in venous cerebral blood volume (CBV) in response to functional tasks. This study used a double-echo gradient echo EPI scheme in conjunction with a graded isocapnic hyperoxic sequence to assess quantitatively the relationship between the fractional venous blood oxygenation ($1\text{-}Y_v$) and transverse relaxation rate of grey matter ($\Delta R_{2\,GM}^*$), without inducing a change in vCBV.

The results demonstrate that the relationship between ΔR_2^* and fractional venous oxygenation at all magnet field strengths studied was adequately described by a linear

relationship. The gradient of this relationship did not increase monotonically with field strength, which may be attributed to the relative contributions of intravascular and extravascular signals which will vary with both field strength and blood oxygenation.

Key words: calibrated BOLD, fMRI, R_2^* quantification, oxygenation, hyperoxia.

1. Introduction

The blood oxygenation level dependent (BOLD) signal arises from the interplay between cerebral blood flow (CBF) and the cerebral metabolic rate of oxygen ($CMRO_2$) consumption. However, the magnitude of the BOLD signal also depends on baseline physiological parameters such as cerebral blood volume (CBV), oxygen extraction fraction (OEF) and haematocrit (Hct) (Kim et al., 2012; Levin et al., 2001; Lin et al., 1998). These parameters can vary for a given individual across repeated scan sessions, between healthy subjects, and in particular across patient groups. This results in variability in the magnitude of the BOLD signal, which can be minimised by using the calibrated BOLD signal to measure changes in the $CMRO_2$ non-invasively. The original calibrated BOLD model of Davis et al. (1998) provides a non-invasive method to quantify the fractional change in cerebral metabolic rate of oxygen ($CMRO_2$) by using the vasodilatory effect of hypercapnia to normalise the BOLD signal.

Current models of calibrated BOLD depend on the relationship between the apparent transverse relaxation rate (R_2^*) and concentration of deoxyhaemoglobin (*dHb*) in the blood, or fractional venous oxygenation ($1\text{-}Y_v$) (Ogawa et al., 1993). The contribution to

R_2^* from deoxygenated blood (ΔR_2^*) can be described as a function of venous CBV (*vCBV*) and blood concentration of *dHb*,

$$\Delta R_2^* = kvCBV[dHb]^\beta \qquad \textbf{Equation 1}$$

where [*dHb*] is a function of OEF and Hct (Davis et al., 1998), and *k* is a constant incorporating properties such as vessel geometry, magnet field strength (B_0) and blood-tissue susceptibility differences.

The parameter β has traditionally been predicted from Monte Carlo simulations and analytical models (Boxerman et al., 1995; He et al., 2007; Ogawa et al., 1993; Yablonskiy et al., 1994). This involves modelling the microscopic magnetic field gradients between deoxygenated blood vessels and the surrounding diamagnetic tissue to estimate the resulting enhancement of the R_2^* decay rate. For the extravascular (EV) compartment, the result depends on whether the system is in the static dephasing regime (larger vessels, $\beta \rightarrow 1$) or the diffusive dephasing regime (smaller vessels, $\beta \rightarrow 2$). The vessel size limit where the transition between these regimes occurs reduces as B_0 increases (Kennan et al., 1994), such that Monte Carlo simulations predict the widely accepted value of β = 1.5 for a vascular network at 1.5 T, and β = 1 at 7 T (Boxerman et al., 1995; Ogawa et al., 1993; Yablonskiy et al., 1994). However, the reliability of these results depends on how realistic the model is. In particular, models should also consider the effect of changes in intravascular (IV) signal contributions due to concomitant changes in vCBV, for example due to vessel dilation in response to functional activation or hypercapnia, and vessel constriction in response to non-isocapnic hyperoxia. This IV contribution can be significant as the R_2^* of blood increases quadratically with increasing deoxygenation (Blockley et al., 2012; Li et al., 1998). At fields below 3 T the intravascular signal from the veins represents a significant fraction of the BOLD signal, estimated to be approximately 57 % at 1.5 T, 36 % at 3 T, and negligible at 7 T (Uludag et al., 2009; van der Zwaag et al., 2009), depending on echo time.

More recently, experimental measurements of β have been published (Driver et al., 2010; Rossi et al., 2012; van der Zwaag et al., 2009; Wise et al., 2013), which are in reasonable agreement with model-based predictions. However, while theoretical estimates may not fully account for intravascular (IV) signal contributions, experimental measurements to date have been subject to potential concomitant changes in vCBV, arising from vessel dilation in response to functional activation or hypercapnia, or vessel constriction in response to non-isocapnic hyperoxia.

This study aims to measure the relationship between fractional change in concentration of deoxyhaemoglobin in venous blood and grey matter R_2^*, without a confounding change in vCBV, using a dynamic isocapnic hyperoxic stimulus at 1.5, 3 and 7 T.

1. Material and Methods

The study was approved by the University of Nottingham Medical School Ethics Committee and all subjects gave prior informed written consent. Eight healthy volunteers (aged 24-27 years, 5 male) participated in the study. MR data was collected on Philips Achieva systems at three B_0s, a 1.5 T system with 8-channel SENSE receive coil, a 3 T system with 32-channel SENSE receive coil and a 7 T system with head volume transmit and 32-channel SENSE receive coil.

An isocapnic hyperoxic stimulus was delivered to subjects using a feed-forward, low gas flow system (RespirAct™, Thornhill Research Inc., Toronto, Canada) in which arterial blood gases were controlled by a prospective targeting system consisting of a computerized gas blender and sequential gas delivery breathing circuit. The system uses the method of Slessarev *et al*. (2007) to target end-tidal PCO_2 ($P_{ET}CO_2$) and PO_2 ($P_{ET}O_2$) independently of each other and independent of breathing pattern (Fierstra et al., 2013). Subjects received medical air via the RespirAct™ until the respiratory

challenge commenced. The respiratory paradigm consisted of three minutes of normocapnic (maintaining $P_{ET}CO_2$ at resting levels) normoxia, followed by a 4 minute normocapnic linear increase in $P_{ET}O_2$ to a maximum level of 500 mmHg (an approximate 8 mmHg increase in $P_{ET}O_2$ with each breath), a linear decrease in $P_{ET}O_2$ to return to baseline over 4 minutes while continuing to maintain normocapnia, and a final 1 minute of normocapnic normoxia. The total respiratory paradigm was thus 12 minutes in duration.

Double echo gradient echo EPI (GE-EPI) data were acquired throughout the respiratory paradigm. At all three magnet field strengths, five contiguous axial slices positioned superior to the ventricles were acquired, with an in-plane resolution of 2×2 mm^3, 3 mm slice thickness, and field of view of 212×188×15 mm^3, 212×184×15 mm^3 and 192×192×15 mm^3 at 1.5, 3 and7 T respectively. Imaging parameters were TR of 3 s, SENSE factor 2.5, flip angle 90°, and TE_1/TE_2 of 25/80 ms, 22/60 ms and 16/47 ms at 1.5, 3 and 7 T respectively. These double echo GE-EPI echo times were selected to optimally fit T_2^* based on the expected grey matter T_2^* value at each B_0, as reported in Peters et al. (2007). In addition, at normoxia, a series of inversion recovery GE-EPI images were acquired at 10 inversion times (100, 200, 300, 500, 700, 1000, 1300, 1500, 2100 and 2600 ms) with matched geometry to the double echo GE-EPI data, which were fit for longitudinal relaxation time, T_1. The first echo (TE_1) images of the double echo GE-EPI datasets were motion corrected using MCFLIRT (FSL, fMRIB, Oxford, UK) and the resulting transforms were applied to the second echo (TE_2) images. A grey matter (GM) mask was formed by thresholding T_1 maps at $1.0 \leq T_1 \leq 1.3$ s, $1.45 \leq T_1 \leq 1.75$ s, and $1.8 \leq T_1 \leq 2.1$ s for 1.5, 3 and 7 T respectively. To remove any remaining contributions in the GM mask from cerebral spinal fluid (CSF) and large veins, those voxels with highest and lowest 3% of signal intensity respectively in the second echo (TE_2) GE-EPI images were removed from the GM mask. R_2^* maps were then calculated within the GM mask on a voxel-wise basis using

$$R_2^* = \frac{1}{TE_2 - TE_1} ln\left(\frac{S_1}{S_2}\right) \qquad \textbf{Equation 2}$$

where S_1 and S_2 denote the signals measured at TE_1 and TE_2. The mean baseline R_2^* was then estimated for the GM mask from the normoxic period, and the baseline R_2^* subtracted from each R_2^* value on hyperoxia, to obtain a timeseries of $\Delta R_{2\,GM}^*$.

The $P_{ET}O_2$ trace was linearly interpolated to a TR of 3 s and $P_{ET}O_2$ measurements were converted to venous oxygenation (Y_v), assuming a baseline OEF of 0.4 (Chiarelli et al., 2007). Y_v values were binned across the full theoretical range of 0.6 to 0.7, in steps of 0.025 to enable the corresponding $R_{2\,GM}^*$ data to be group averaged over these bins. For each individual subjects' data, at each B_0, the average value of $\Delta R_{2\,GM}^*$ within the GM mask was fitted to two models. First, a simple linear function

$$\Delta R_{2\,GM}^* = A(1 - Y_v) + C \qquad \textbf{Equation 3}$$

where $(1\text{-}Y_v)$ *is* proportional to [*dHb*] in Equation 1, and A and C are the fitted gradient and intercept (which takes account of the fact that we do not measure $\Delta R_{2\,GM}^*$ with respect to $Y_v = 0$). Second, to a power law function

$$\Delta R_{2\,GM}^* = A'(1 - Y_v)^{\beta} + C' \qquad \textbf{Equation 4}$$

to estimate A', β and C', using a non-linear, three parameter least squares fit. Data were also fitted to Equation 4, fixing β to published B_0-corrected values (1.5, 1.3 and 1 for 1.5T, 3T and 7T respectively (Bulte et al., 2009; Davis et al., 1998; Driver et al., 2012)). The Chi-squared (X^2) was used as a measure of the goodness of fit.

We also simulated the relationship between the EV signal and venous oxygenation by using the known blood deoxyhaemoglobin relaxivity to separate the IV component from the total tissue signal, to explore contributions of any residual IV signal which was not accounted for by removal of voxels containing large vessels. While the intravascular relaxation rate $R_{2\,IV}^*$ varies quadratically with $(1\text{-}Y_v)$ (Blockley et al., 2008; Li et al., 1998)

a linear relationship was assumed across the range of venous oxygenation targeted in this study (0.6-0.7) (Blockley et al., 2008). The resulting estimates of $R_{2\,IV}^{*}$ were combined with the measured values of ΔR_{2*GM} to estimate the variations in ΔR_{2*EV}. First a simple two compartment model was assumed:

$$S_{voxel} = M_0\left(f_v.e^{-TE.R_{2\,IV}^{*}} + (1-f_v).e^{-TE.R_{2\,EV}^{*}}\right) \qquad \textbf{Equation 5}$$

where S_{voxel} is the GM signal measured from a voxel at echo time TE, f_v is intravascular blood volume fraction (assumed to be 3% (Helenius et al., 2003; Lee et al., 2001)) and $R_{2\,IV}^{*}$ and $R_{2\,EV}^{*}$ correspond to the R_2^{*} of the IV and EV compartments respectively, neglecting vessel orientation effects. The ratio of the signal measured at echo times TE_1 and TE_2 can then be written as:

$$\frac{S_1}{S_2} = \frac{f_v.e^{-TE_1.R_{2\,IV}^{*}} + (1-f_v).e^{-TE_1.R_{2\,EV}^{*}}}{f_v.e^{-TE_2.R_{2\,IV}^{*}} + (1-f_v).e^{-TE_2.R_{2\,EV}^{*}}}, \qquad \textbf{Equation 6}$$

Assuming that $\Delta R_{2\,EV}^{*}$ also varied linearly with Y over the range of interest and a literature value of f, the variation in S_1/S_2 versus $(1\text{-}Y_v)$ was fitted to determine the expected values of $\Delta R_{2\,EV}^{*}$. In this simulation the differences in T_1 and spin density between tissue and blood were assumed negligible; in fact tissue possesses a slightly lower spin density and shorter T_1 than blood so these effects will work in opposing directions.

3. Results

Average baseline and peak $P_{ET}O_2$ values achieved at each B_0 are shown in Table 1, along with the corresponding Y_v value. Group averaged $P_{ET}O_2$ traces are shown in Figure 1A-C. $P_{ET}CO_2$ values were maintained within ± 0.39 mmHg of an individuals' resting level, with the mean change between baseline normoxia and peak hyperoxia being 0.70 ± 0.12 mmHg, across all subjects and B_0. Such fluctuations in $P_{ET}CO_2$ were assumed to have minimal influence on R_2^{*}. Baseline (normoxic) $R_{2\,GM}^{*}$ increased

significantly with B_0 ($p < 0.005$, Wilcoxon signed rank test). Example Y_v and $\Delta R_2^*{}_{GM}$ timecourses are shown for representative subjects across B_0 in Figures 1D-F. Corresponding maps of R_2^* and the gradient (A) of the linear fit to Equation 3 are depicted in Figure 2.

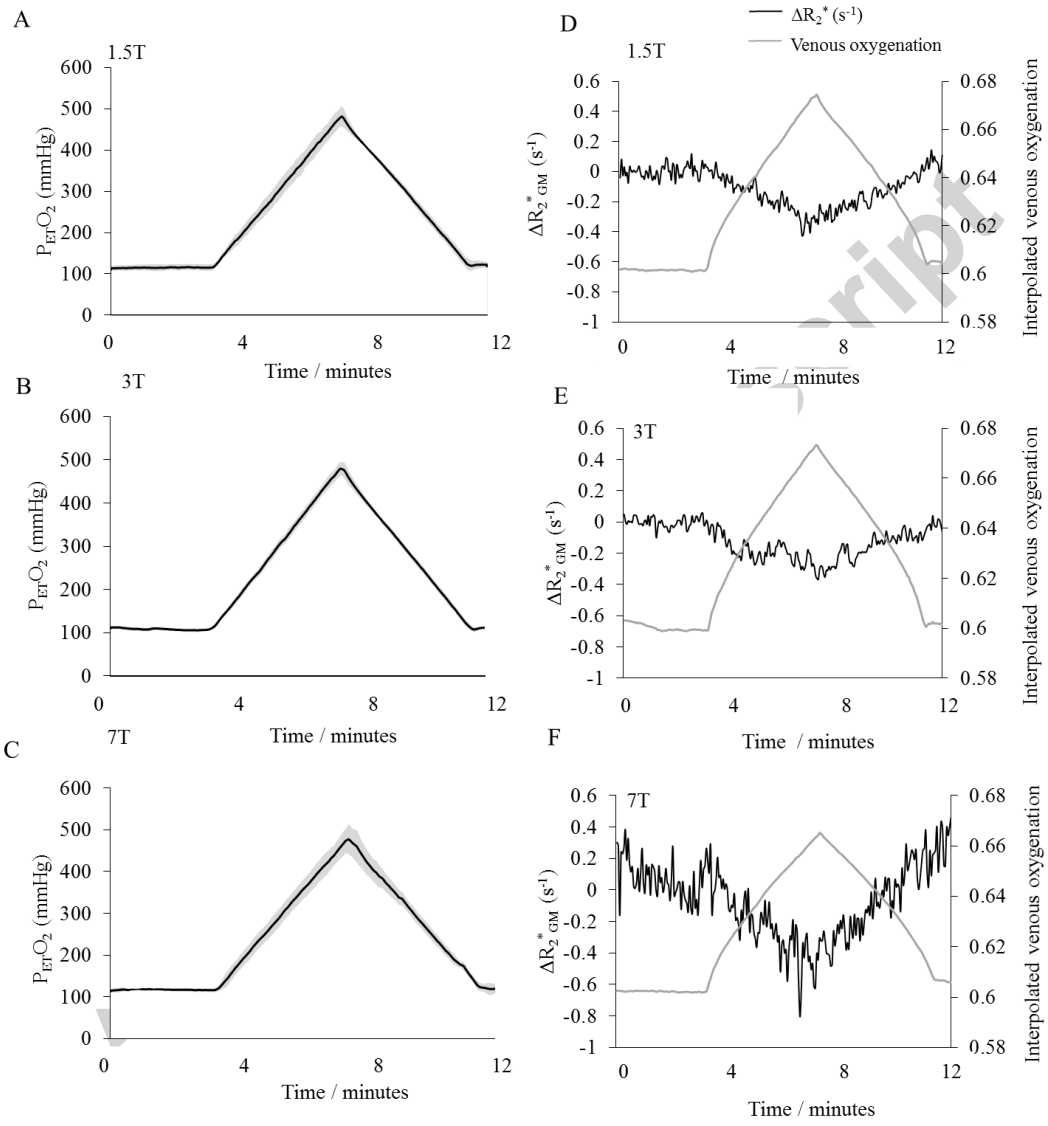

Figure 1: A-C) Group averages of end tidal partial pressure of oxygen ($P_{ET}O_2$) shown in black at each field strength across the twelve minute respiratory paradigm. Grey regions indicate standard deviation. D-F) Interpolated venous

oxygenation (Y_v) time course for representative subjects and accompanying ΔR_2^* (s^{-1}) at B) 1.5 T, C) 3 T and D) 7 T.

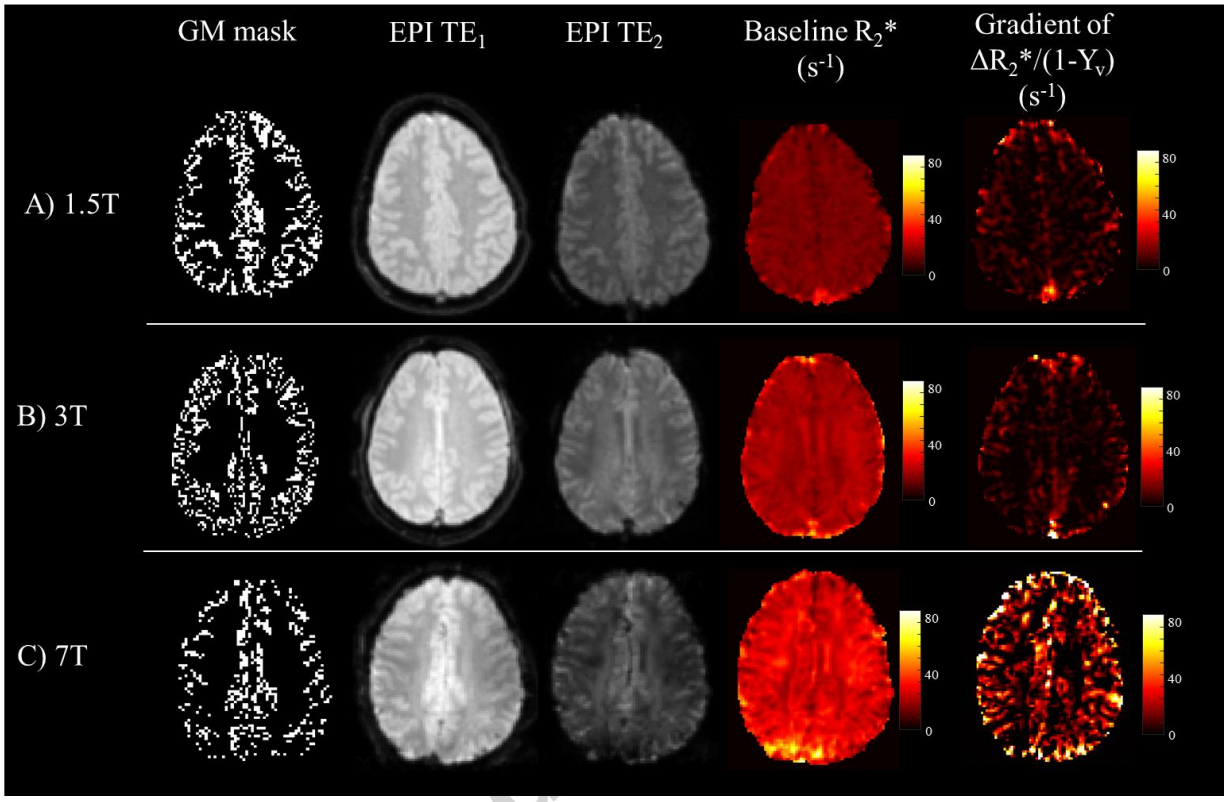

Figure 2: Grey matter (GM) masks, EPIs for TE_1 and TE_2 at normoxic baseline, with corresponding R_2^* images, and voxelwise gradient of $\Delta R_{2\,GM}^*$ versus $(1-Y_v)$. Data shown for representative subjects at A) 1.5 T, B) 3 T and C) 7 T.

Figure 3A shows the effect of the fractional change in venous oxygenation ($1-Y_v$) on $\Delta R_{2\,GM}^*$ for each B_0. The average gradient, A, of the linear fit of $\Delta R_{2\,GM}^*$ versus $(1-Y_v)$ (Equation 3) is given in Table 1. This was significantly larger for 7 T than 1.5 or 3 T ($p = 0.043$, Kruskall-Wallis one-way ANOVA), although no significant difference was observed between 1.5 and 3 T.

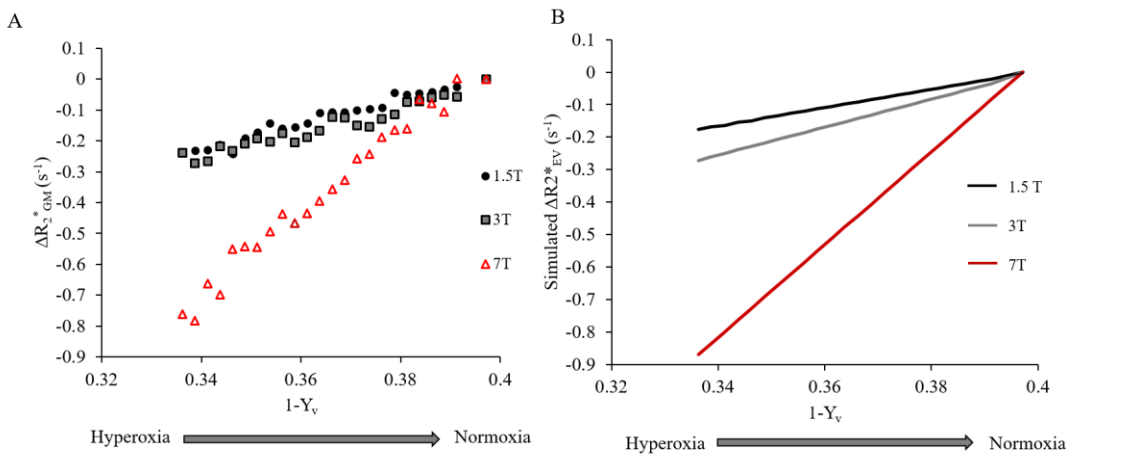

Figure 3: A) Effect of change in fractional venous oxygenation (1-Y_v) on A) $\Delta R_2^*{}_{GM}$ (s^{-1}) and B) $\Delta R_2^*{}_{EV}$ (s^{-1}), shown at 1.5 T (black), 3 T (grey) and 7 T (red). Data binned and averaged across subjects.

The data was sufficiently described by the linear 2 parameter (A and C) model fit (Equation 3) ($p < 0.01$ in all cases). The 3 parameter model, showed no significant improvements in goodness-of-fit (X^2 Difference test) when compared to either of the 2 parameter fits (linear, and fixed B_0-corrected values of β).

When R_2*_{EV} was estimated across binned Y_v values based on the measured signals and estimated R_2*_{IV}, the results demonstrated a monotonic increase in the gradient of $\Delta R_2^*{}_{EV}$ and (1-Y_v) with B_0 (Figure 3B). Figure 4 illustrates subsequent intravascular and extravascular GM signal components for the echo times and field strengths used in this study, for both normoxia and hyperoxia, using Equation 5.

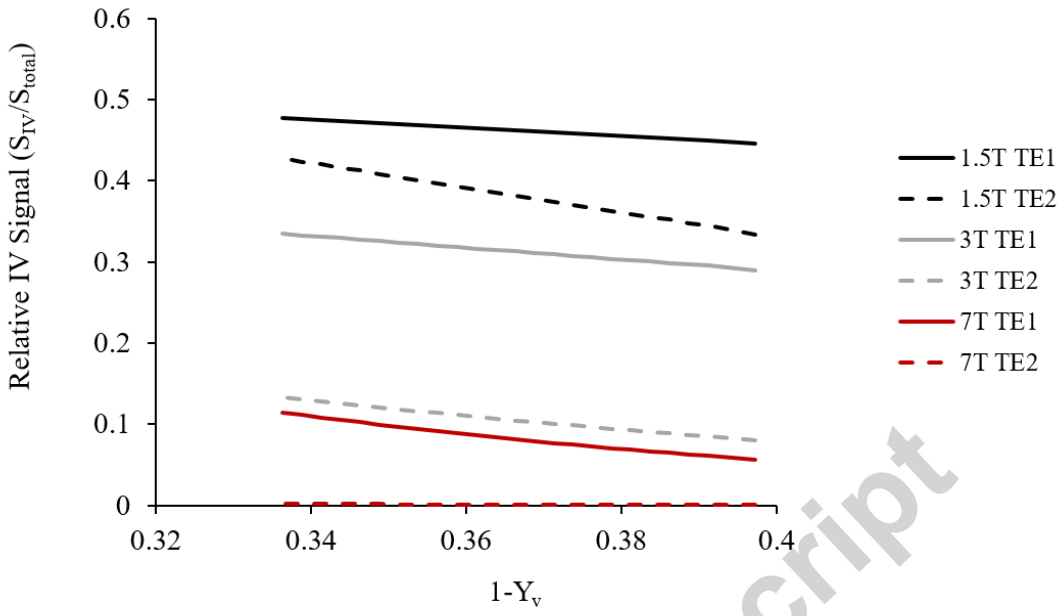

Figure 4: Variation in relative IV signal contribution with (1-Y_v) estimated for each echo time and field strength.

4. Discussion

The relationship between $\Delta R_{2}^{*}{}_{GM}$ and fractional venous oxygenation ($1\text{-}Y_v$) was measured at 1.5, 3 and 7 T, and found to be well-described by a linear relationship at all B_0s. This contrasts with previous studies which inferred that $\beta \geq 1$ by manipulating B_0 (Driver et al., 2010; Rossi et al., 2012; van der Zwaag et al., 2009), and by the direct measurement of a value of β of 1.35 at 3 T using the response to combined hyperoxia and hypercapnia (Wise et al., 2013). In our study β was measured using an isocapnic hyperoxic stimulus and so the results are not confounded by changes in vCBV which will have occurred in previous studies, with vCBV altered by motor activation (van der Zwaag et al., 2009), the vasodilative effect of hypercapnia (Driver et al., 2010; Wise et al., 2013) or non-isocapnic hyperoxia (Rossi et al., 2012).

Baseline $R_{2\,GM}^{*}$ increased monotonically and approximately linearly with B_0, in agreement with published cross-field values (Rossi et al., 2012; van der Zwaag et al., 2009). In contrast, the gradient of $\Delta R_{2\,GM}^{*}$ versus (1-Y_v) measured in this study did not increase monotonically (Figure 3). Extravascular dephasing depends on the intravascular frequency shift ($\Delta\omega$), which depends linearly on both (1-Y_v) and B_0:

$$\Delta\omega = k''.\gamma.B_0.\Delta\chi.(1-Y_v) \qquad \textbf{Equation 7}$$

where *k"* is a constant reflecting vessel geometry, γ is the gyromagnetic ratio and $\Delta\chi$ is the difference in magnetic susceptibility between fully deoxygenated blood and tissue. Therefore, if we were only sensitive to extravascular signal in the static or indeed diffusive regimes, the gradient of $\Delta R_{2\,GM}^{*}$ versus (1-Y_v) would be expected to increase monotonically with B_0 (Boxerman et al., 1995; Ogawa et al., 1993; Yablonskiy et al., 1994). In practice, the gradient was effectively constant between 1.5 and 3 T and increased faster than linearly with B_0 between 3 and 7 T (Table 1).

In practice, the non-negligible intravascular (IV) signal will contribute to the signal from GM (Hare et al., 2016), even when signal from large vessels has been masked out, as was the case in this work. Therefore, the unexpected variation in the gradient of $\Delta R_{2\,GM}^{*}$ versus (1-Y_v) with B_0 might be explained by a variation in the ratio of IV signal to EV signal contributions with both B_0 and echo time (*TE*). Here we combined measured values of $\Delta R_{2\,GM}^{*}$ with previously published values of $R_{2\,IV}^{*}$ to estimate $\Delta R_{2\,EV}^{*}$, and the results indicated that the gradient of $\Delta R_{2\,EV}^{*}$ versus (1-Y_v) increased monotonically with B_0 as expected (Boxerman et al., 1995; Ogawa et al., 1993; Yablonskiy et al., 1994).

If a multi-compartment signal decay is fitted to a single exponential, the apparent R_2^{*} will depend on the choice of echo times at which the signal is sampled. Figure 4 illustrates

how the estimated relative contribution of intravascular signal to total signal varies with oxygenation and field strength for the T_2* values measured here. The IV signal is smaller at normoxia than at hyperoxia, and therefore contributes less to the total signal as (1-Y_v) increases. Furthermore, for the echo times used here, the IV signal is more sensitive to changes in fractional venous oxygenation than the EV signal, particularly at lower field. This varying intravascaular signal contribution may explain the unexpected variation of the gradient of $\Delta R_{2\,GM}^{*}$ versus (1-Y_v) with B_0. However, it should also be noted that any trends in the gradient of a linear fit over a limited range of (1-Y_v) could be hard to interpret if the underlying function was not in fact linear. Future studies designed specifically to explore these relationships should use a multi-echo EPI readout and vascular crushing to separate the different IV and EV compartments. In this study the frequency offset ($\Delta\omega$) between tissue and blood was varied by changing both venous oxygenation and B_0. To fully characterise the dependency of grey matter R_2^* on $\Delta\omega$, a larger intravascular susceptibility perturbation is required, either by modulating venous blood oxygenation over a wider range, which is difficult to achieve physiologically, or by using a paramagnetic contrast agent.

In summary if the underlying physical value of β for any compartment is non-linear, then the effective value of β will depend on experimental parameters and local tissue microvasculature (Griffeth et al., 2011; Martindale et al., 2008), but for calibrated BOLD an additional experiment to determine β would be impractical. However for the experimental protocol used here, which was deliberately characteristic of standard fMRI experiments, a linear approximation was sufficient to describe the observed behaviour across the limited range of (1-Y_v) = 0.3-0.4 relevant to the fMRI BOLD effect at all field strengths, which could simplify the calibration of the BOLD signal (Blockley et al., 2015; Griffeth et al., 2013; Merola et al., 2016). Recent work (Griffeth et al., 2011; Merola et al., 2016) has tested calibrated BOLD models by comparing the relatively simple BOLD signal models with a more detailed, multi-compartment BOLD signal model, treating this more detailed model as a gold standard from which to test the specificity of the calibrated BOLD approach to simulated data. The main conclusion of this work was that

the physical meaning of the parameter β (alongside a physiological CBV/CBF coupling parameter) should be relaxed and their values treated as free parameters.

It has previously been shown that a strong hyperoxic stimulus (FiO_2 = 1) will cause macroscopic alterations in inferior brain regions at 3T which can increase the measured R_2*, although such effects were reduced under moderate hyperoxia (FiO_2 = 0.5) (Pilkinton et al., 2011). Similarly at 7 T, we have previously observed whole-head field shifts under moderate hyperoxia (~FiO_2 = 0.6, $P_{ET}O_2$ = 500mmHg), although this only resulted in significant changes in R_2^* in regions close to the frontal sinus (Driver et al., 2011). In this work such macroscopic effects were mitigated by selecting slices superior to the ventricles, and using moderate hyperoxia. Nonetheless, further quantification of macroscopic inhomogeneities caused by hyperoxia and their impact on R_2^* are required to enable whole-head analysis. Furthermore, a different paradigm (e.g. sinusoidal (Blockley et al., 2010)) would make it easier to remove any drifts from the data.

5. Conclusions

This work presents the first experimental measurement of β in humans using an isocapnic hyperoxic stimulus to remove confounds associated with a change in CBV arising from functional activation or modulation of $P_{ET}O_2$ during a respiratory challenge. It was also found that for the regimes relevant to calibrated BOLD experiments, a value of β=1 is a reasonable assumption, which may help simplify the calibrated BOLD model.

Acknowledgements:

We wish to thank Dr. Emma Hall for her assistance with data acquisition and analysis. This work was funded by The University of Nottingham and The Medical Research Council

References

Blockley, N., Driver, I. D., Fisher, J. A., Francis, S. T., & Gowland, P. A. (2012). Measuring venous blood volume changes during activation using hyperoxia. *Neuroimage*, *59*(4), 3266–3274.

Blockley, N., Driver, I. D., Francis, S. T., Fisher, J. a., & Gowland, P. A. (2010). An improved method for acquiring cerebrovascular reactivity maps. *Neuroimage*, *65*(5), 1278–86.

Blockley, N., Griffeth, V., Stone, A., Hare, H., & Bulte, D. (2015). Sources of systematic error in calibrated BOLD based mapping of baseline oxygen extraction fraction. *NeuroImage*, *122*, 105–113. doi:10.1016/j.neuroimage.2015.07.059

Blockley, N., Jiang, L., Gardener, A., Ludman, C. N., Francis, S. T., & Gowland, P. a. (2008). Field strength dependence of R1 and R2* relaxivities of human whole blood to ProHance, Vasovist, and deoxyhemoglobin. *Magnetic Resonance in Medicine : Official Journal of the Society of Magnetic Resonance in Medicine / Society of Magnetic Resonance in Medicine*, *60*(6), 1313–20. doi:10.1002/mrm.21792

Boxerman, J. L., Hamberg, L. M., Rosen, B. R., & Weisskoff, R. M. (1995). Mr contrast due to intravascular magnetic susceptibility perturbations. *Magnetic Resonance in Medicine*, *34*(4), 555–566. doi:10.1002/mrm.1910340412

Bulte, D. P., Drescher, K., & Jezzard, P. (2009). Comparison of hypercapnia based calibration techniques for measurement of cerebral oxygen metabolism with MRI. *Magnetic Resonance in Medicine*, *61*(2), 391–398.

Chiarelli, P. A., Bulte, D. P., Wise, R., Gallichan, D., & Jezzard, P. (2007). A calibration method for quantitative BOLD fMRI based on hyperoxia. *Neuroimage*, *37*(3), 808–820.

Davis, T. L., Kwong, K. K., Weisskoff, R. M., & Rosen, B. R. (1998). Calibrated functional MRI: mapping the dynamics of oxidative metabolism. *Proceedings of the National Academy of Sciences of the United States of America*, *95*(4), 1834–1839.

Driver, I., Blockley, N., Fisher, J., Francis, S., & Gowland, P. (2010). The change in cerebrovascular reactivity between 3 T and 7 T measured using graded hypercapnia. *NeuroImage*, *51*(1), 274–9. doi:10.1016/j.neuroimage.2009.12.113

Driver, I., Hall, E., Wharton, S., Pritchard, S., Francis, S., & Gowland, P. (2012). Calibrated BOLD using direct measurement of changes in venous oxygenation. *NeuroImage*, *63*(3), 1178–87. doi:10.1016/j.neuroimage.2012.08.045

Driver, I., Harmer, J., Hall, E., Pritchard, S., Francis, S., & Gowland, P. (2011). Quantifying the artefacts caused by hyperoxic challenges. *Proc. Intl. Soc. Mag. Reson. Med*.

Fierstra, J., Sobczyk, O., Battisti-Charbonney, a, Mandell, D. M., Poublanc, J., Crawley, a P., … Fisher, J. a. (2013). Measuring cerebrovascular reactivity: what stimulus to use? *The Journal of Physiology*, *591*(Pt 23), 5809–21. doi:10.1113/jphysiol.2013.259150

Griffeth, V. E. M., Blockley, N. P., Simon, A. B., & Buxton, R. B. (2013). A New

Functional MRI Approach for Investigating Modulations of Brain Oxygen Metabolism. *PLoS ONE*, *8*(6), 1–13. doi:10.1371/journal.pone.0068122

Griffeth, V. E. M., & Buxton, R. B. (2011). A theoretical framework for estimating cerebral oxygen metabolism changes using the calibrated-BOLD method: modeling the effects of blood volume distribution, hematocrit, oxygen extraction fraction, and tissue signal properties on the BOLD signal. *NeuroImage*, *58*(1), 198–212. doi:10.1016/j.neuroimage.2011.05.077

Hare, H. V, & Bulte, D. P. (2016). Investigating the Dependence of the Calibration Parameter M on Echo Time, *561*, 556–561. doi:10.1002/mrm.25603

He, X., & Yablonskiy, D. A. (2007). Quantitative BOLD: Mapping of human cerebral deoxygenated blood volume and oxygen extraction fraction: Default state. *Magnetic Resonance in Medicine*, *57*(1), 115–126. doi:10.1002/mrm.21108

Helenius, J., Perkiö, J., Soinne, L., Østergaard, L., Carano, R. A. D., Salonen, O., … Tatlisumak, T. (2003). Cerebral hemodynamics in a healthy population measured by dynamic susceptibility contrast MR imaging. *Acta Radiologica (Stockholm, Sweden : 1987)*, *44*(5), 538–46. Retrieved from http://www.ncbi.nlm.nih.gov/pubmed/14510762

Kennan, R. P., Zhong, J., & Gore, J. C. (1994). Intravascular susceptibility contrast mechanisms in tissues. *Magnetic Resonance in Medicine*, *31*(1), 9–21. doi:10.1002/mrm.1910310103

Kim, S., & Ogawa, S. (2012). Biophysical and physiological origins of blood oxygenation level-dependent fMRI signals. *Journal of Cerebral Blood Flow & Metabolism*, *32*(7), 1188–1206. doi:10.1038/jcbfm.2012.23

Lee, S. P., Duong, T. Q., Yang, G., Iadecola, C., & Kim, S. G. (2001). Relative changes of cerebral arterial and venous blood volumes during increased cerebral blood flow: implications for BOLD fMRI. *Magnetic Resonance in Medicine*, *45*(5), 791–800.

Levin, J., deB Frederick, B., Ross, M., Fox, J., von Rosenberg, H., Kaufman, M., … Renshaw, P. (2001). Influence of baseline hematocrit and hemodilution on BOLD fMRI activation. *Magnetic Resonance Imaging*, *19*(8), 1055–1062.

Li, D., Waight, D. J., & Wang, Y. (1998). In vivo correlation between blood T2* and oxygen saturation. *Journal of Magnetic Resonance Imaging : JMRI*, *8*(6), 1236–9. Retrieved from http://www.ncbi.nlm.nih.gov/pubmed/9848734

Lin, W., RP, P., Celik, A., Hsu, C., & Powers, W. (1998). Effects of acute normovolemic hemodilution on T2*-weighted images of rat brain. *Magnetic Resonance in Medicine*, *40*(6), 857–64.

Martindale, J., Kennerley, A. J., Johnston, D., Zheng, Y., & Mayhew, J. E. (2008). Theory and generalization of Monte Carlo models of the BOLD signal source. *Magnetic Resonance in Medicine : Official Journal of the Society of Magnetic Resonance in Medicine / Society of Magnetic Resonance in Medicine*, *59*(3), 607–18. doi:10.1002/mrm.21512

Merola, A., Murphy, K., Stone, A. J., Germuska, M. A., Griffeth, V. E. M., Blockley, N. P., … Wise, R. G. (2016). NeuroImage Measurement of oxygen extraction fraction (

OEF): An optimized BOLD signal model for use with hypercapnic and hyperoxic calibration. *NeuroImage*, *129*, 159–174. doi:10.1016/j.neuroimage.2016.01.021

Ogawa, S., Menon, R. S., Tank, D. W., Kim, S. G., Merkle, H., Ellermann, J. M., & Ugurbil, K. (1993). Functional brain mapping by blood oxygenation level-dependent contrast magnetic resonance imaging. A comparison of signal characteristics with a biophysical model. *Biophysical Journal*, *64*(3), 803–812.

Peters, A. M., Brookes, M. J., Hoogenraad, F. G., Gowland, P. A., Francis, S. T., Morris, P. G., & Bowtell, R. (2007). T2* measurements in human brain at 1.5, 3 and 7 T. *Magnetic Resonance Imaging*, *25*(6), 748–753. doi:10.1016/j.mri.2007.02.014

Pilkinton, D. T., Gaddam, S. R., & Reddy, R. (2011). Characterization of paramagnetic effects of molecular oxygen on blood oxygenation level-dependent-modulated hyperoxic contrast studies of the human brain. *Magnetic Resonance in Medicine*, *66*(3), 794–801. doi:10.1002/mrm.22870

Rossi, C., Boss, A., Donati, O. F., Luechinger, R., Kollias, S. S., Valavanis, A., … Nanz, D. (2012). Manipulation of cortical gray matter oxygenation by hyperoxic respiratory challenge: field dependence of R(2) * and MR signal response. *NMR in Biomedicine*, *25*(8), 1007–14. doi:10.1002/nbm.2775

Slessarev, M., Han, J., Mardimae, A., Prisman, E., Preiss, D., Volgyesi, G., … Fisher, J. A. (2007). Prospective targeting and control of end-tidal CO2 and O2 concentrations. *The Journal of Physiology*, *581*(3), 1207–1219.

Uludag, K., Müller-bierl, B., & Ugurbil, K. (2009). An integrative model for neuronal activity-induced signal changes for gradient and spin echo functional imaging. *NeuroImage*, *48*(1), 150–165. doi:10.1016/j.neuroimage.2009.05.051

van der Zwaag, W., Francis, S., Head, K., Peters, A., Gowland, P., Morris, P., & Bowtell, R. (2009). fMRI at 1.5, 3 and 7 T: characterising BOLD signal changes. *NeuroImage*, *47*(4), 1425–34. doi:10.1016/j.neuroimage.2009.05.015

Wise, R. G., Harris, A. D., Stone, A., & Murphy, K. (2013). Measurement of OEF and absolute CMRO 2 : MRI-based methods using interleaved and combined hypercapnia and hyperoxia. *Neuroimage*, *83*, 135–147. doi:10.1016/j.neuroimage.2013.06.008.Measurement

Yablonskiy, D. A., & Haacke, E. M. (1994). Theory of NMR signal behavior in magnetically inhomogeneous tissues: the static dephasing regime. *Magnetic Resonance in Medicine*, *32*(6), 749–763.

Table 1: Average baseline and peak $P_{ET}O_2$ values and corresponding venous oxygenation (Y_v) estimated according to the interpolation method outlined in Chiarelli et al. (2007). Baseline $R_2^*{}_{GM}$ (s^{-1}) and the gradients (A) of $\Delta R_2^*{}_{GM}$ versus ($1-Y_v$) for both β = 1 (linear model) and typical B_0-adjusted values of β. X^2 depicts goodness-of-fit. Data (mean ± SEM) averaged across subjects for each magnet field strength (B_0). † denotes p < 0.01.

	$P_{ET}O_2$ (mmHg)		Venous oxygenation (Y_v)		MR parameters for GM mask			
B_0 (T)	Baseline	Peak	Baseline	Peak	Baseline $R_2^*{}_{GM}$ (s^{-1})	Gradient (*A*) of $\Delta R_2^*{}_{GM}$ v. $(1-Y_v)$ linear fit (*Equation 3*) (s^{-1})	X^2 for nonlinear fit using B_0-corrected *β* values (*Equation 4*)	X^2 for nonlinear 3 parameter fit (*Equation 4)*
1.5	115 ± 3	482 ± 11	0.600 ± 0.001	0.670 ± 0.002	12.7 ± 0.2	4.1 ± 0.4 (χ^2 = 6.4 ± 2.0†)	χ^2 = 6.4 ± 2.0†	χ^2 = 6. 4 ± 2.0†
3	109 ± 3	485 ± 9	0.600 ± 0.001	0.680 ± 0.001	19.5 ± 0.5	3.9 ± 0.3 (χ^2 = 4.3 ± 1.1†)	χ^2 = 4.3 ± 1.1†	χ^2 = 4.2 ± 1.8†
7	119 ± 2	490 ± 13	0.600 ± 0.001	0.670 ± 0.003	33.2 ± 0.7	13.2 ± 2.0 (χ^2 = 4.7 ± 1.8†)	χ^2 = 4.7 ± 1.8†	χ^2 = 4.6 ± 1.8†

Highlights

- We assess the relationship between grey matter R2* and venous oxygenation
- Isocapnic hyperoxia prevented confounding changes in cerebral blood volume
- A linear dependency is an appropriate assumption at 1.5, 3 and 7 Tesla
- Intravascular/extravascular signal ratios will vary with both B_0 and oxygenation